Caveolae/lipid rafts in fibroblast-like synoviocytes: ectopeptidase-rich membrane microdomains

Dagmar RIEMANN*, Gert H. HANSEN†, Lise-Lotte NIELS-CHRISTIANSEN†, Evy THORSEN†, Lissi IMMERDAL†, Alexander Navarrete SANTOS*, Astrid KEHLEN*, Jürgen LANGNER* and E. Michael DANIELSEN†[1]

*Institute of Medical Immunology, Martin Luther University, Halle-Wittenberg, Strasse der OdF 6, D-06097 Halle, Germany, and †Department of Medical Biochemistry and Genetics, The Panum Institute, University of Copenhagen, Blegdamsvej 3, DK-2200 Copenhagen N, Denmark

Membrane peptidases play important roles in cell activation, proliferation and communication. Human fibroblast-like synoviocytes express considerable amounts of aminopeptidase N/CD13, dipeptidyl peptidase IV/CD26, and neprilysin/CD10, transmembrane proteins previously proposed to be involved in the regulation of intra-articular levels of neuropeptides and chemotactic mediators as well as in adhesion and cell–cell interactions. Here, we report these peptidases in synoviocytes to be localized predominantly in glycolipid- and cholesterol-rich membrane microdomains known as 'rafts'. At the ultrastructural level, aminopeptidase N/CD13 and dipeptidyl peptidase IV/CD26 were found in caveolae, in particular in intracellular yet surface-connected vesicle-like structures and 'rosettes' made up of several caveolae. In addition, clusters of peptidases were seen at the cell surface in flat patches ranging in size from about 60 to 160 nm. Cholesterol depletion of synoviocytes by methyl-β-cyclodextrin disrupted $> 90\,\%$ of the caveolae and reduced the raft localization of aminopeptidase N/CD13 without affecting Ala-*p*-nitroanilide-cleaving activity of confluent cell cultures. In co-culture experiments with T-lymphocytes, cholesterol depletion of synoviocytes greatly reduced their capability to induce an early lymphocytic expression of aminopeptidase N/CD13. We propose caveolae/rafts to be peptidase-rich 'hot-spot' regions of the synoviocyte plasma membrane required for functional cell–cell interactions with lymphocytes. The peptidases may act in concert with other types of proteins such as receptors and signal transducers localized in these specialized membrane domains.

Key words: aminopeptidase N/CD13, dipeptidyl peptidase IV/CD26, neprilysin/CD10, raft membrane microdomain, synoviocyte.

INTRODUCTION

Fibroblast-like synoviocytes are the prominent cell type in rheumatoid joint pannus tissue and have a central role in the pathogenesis and development of rheumatoid arthritis [1]. They express considerable amounts of peptidases, a multifunctional group of enzymes of which several have been implicated in the control of growth and differentiation of various cellular systems [2–4]. Aminopeptidase N/CD13, the most abundant synoviocyte ectopeptidase, is a widely expressed zinc-dependent enzyme that preferentially catalyses the removal of neutral amino acids from oligopeptides. It is a 160 kDa protein anchored to the cell membrane by a single transmembrane helical region near the N-terminus and with a short cytoplasmic tail of only 8–10 amino acids [5]. The functional significance of the high synoviocyte expression level of aminopeptidase N/CD13 is not fully understood at present, but it represents a cellular potential for inactivation of inflammatory mediators such as neuropeptide hormones [6], kinins [7] and chemotactic substances [8]. In co-culture experiments, synoviocytes rapidly induce a persistent aminopeptidase N/CD13 surface expression on both T- and B-lymphocytes [9]. Interestingly, this induction was observed to require direct cell–cell contact and could not be mimicked by soluble aminopeptidase N, pointing to a more complex role of the ectopeptidase in this process [9].

Other membrane peptidases, such as neprilysin/CD10 and dipeptidyl peptidase IV/CD26, are co-expressed with aminopeptidase N/CD13 in fibroblast-like synoviocytes and seem to co-operate in peptide degradation [2]. Neprilysin/CD10, also referred to as neutral endopeptidase 24.11, enkephalinase and CALLA (common acute lymphoblastic leukaemia antigen), is a ubiquitously occurring membrane-bound zinc-dependent metallopeptidase with a broad functional repertoire. The enzyme has a specificity for cleaving oligopeptides (up to about 40 amino acids in length) preferentially on the amino side of hydrophobic residues. It has been implicated in many physiological processes, such as enkephalin-induced analgesia, atrial natriuretic peptide-mediated hypotension and diuresis, airway tone, down-regulation of neurogenic inflammation and chemotaxis [10]. The serine protease dipeptidyl peptidase IV/CD26 catalyses the release of N-terminal dipeptides from peptides with proline, hydroxyproline or alanine in the penultimate position. It binds to collagen and adenosine deaminase, plays a role in T-cell activation and is implicated in the processing of neuropeptides such as neuropeptide Y and endomorphin, peptide hormones, such as glucagon-like peptides-1 and -2, and chemotactic cytokines, such as RANTES (regulated upon activation, normally T-cell expressed and secreted) and SDF-1 (stromal cell-derived factor 1) [11].

Over the past few years it has become increasingly clear that the lipid bilayer of the plasma membrane of many cell types is organized into microdomains rich in glycosphingolipids and cholesterol, commonly referred to as 'rafts' [12–14]. Rafts are thought to exist as relatively ordered (l_o phase) membrane patches

[1] To whom correspondence should be addressed (e-mail midan@imbg.ku.dk).

surrounded by more fluid, liquid-crystalline (l_c phase) membrane composed mainly of glycerolipids, and to provide a platform for a number of different types of protein, including various receptors, membrane transporters, structural proteins and signal transducers. In some but not all cases, rafts reflect the presence of caveolae, small flask-shaped membrane invaginations at the cell surface engaged in endocytic membrane trafficking as well as in cell signalling events [12–16].

In the present work, we studied in closer detail the subcellular localization and membrane organization of aminopeptidase N/CD13, dipeptidyl peptidase IV/CD26 and neprilysin/CD10 in cultures of rheumatoid synoviocytes. The results obtained demonstrate that these peptidases are localized mainly to raft membrane microdomains morphologically identifiable as caveolae, in particular intracellular yet surface-connected vesicle-like caveolae and caveolae 'rosettes', whereas at the cell surface they mainly cluster in flat patches of about 60–160 nm. Cholesterol depletion disrupted the caveolar/raft organization and greatly reduced the ability of synoviocytes to induce an early lymphocytic expression of aminopeptidase N/CD13. The cell–cell interactions taking place between synoviocytes and lymphocytes therefore seem to rely on a cholesterol-dependent microdomain compartmentation of the synoviocyte cell surface and to involve clustering of membrane peptidases, possibly together with other cell-surface peptidases, receptors and signal-transduction proteins.

EXPERIMENTAL

Materials

Gelatin and Fungizone were purchased from Life Technologies (Eggenstein, Germany). Ala-*p*-nitroanilide, concanavalin A, protease inhibitor mixture and methyl-β-cyclodextrin were from Sigma (St. Louis, MO, U.S.A.). Refobacin was purchased from Merck (Darmstadt, Germany). Interleukin-2 (Proleukin) was obtained from Behring AG (Marburg, Germany). Monoclonal antibodies used: Leu-M7 (CD13), CD3, CD14, CD19 and negative controls IgG1-FITC/IgG2a-phycoerythrin (Becton Dickinson, Heidelberg, Germany), MCA1556 (CD10) (SEROTEC, Kidlington, Oxon, U.K.), MY7 (CD13; Coulter, Hamburg, Germany), WM15 (CD13; Dianova, Hamburg, Germany), SJ1D1 (CD13; Immunotech, Hamburg, Germany) and EBM11 (CD68; Dako, Hamburg, Germany). A polyclonal antibody to caveolin was obtained from Transduction Laboratories (Lexington, KY, U.S.A.). A secondary antibody against mouse IgG (FITC-labelled) and an antibody against rabbit IgG (labelled with Cy3) were purchased from Immunotech. A polyclonal antibody specific for dipeptidyl peptidase IV was kindly provided by U. Kettmann (Institute of Physiological Chemistry, Martin Luther University, Halle, Germany). The use of an antibody to intestinal aminopeptidase N for immunoblotting and immunogold electron microscopy has been described elsewhere [17].

Cell isolation and culture

Fibroblast-like synoviocytes were isolated from the adherent cells of collagenase-dispersed synovectomy tissues of patients suffering from juvenile chronic arthritis or rheumatoid arthritis as reported previously [3]. The use of joint pannus as a source of synoviocytes was performed with the permission of the local ethics committee. The cells were grown in Dulbecco's modified Eagle's medium (Gibco-BRL, Paisley, Scotland, U.K.), containing 10 % foetal calf serum and antibiotics, in flasks precoated with 0.5 % gelatin. Cells were passaged with 0.2 mM EDTA and 0.05 % trypsin. Experiments were performed using confluent cell lines of the third to eleventh passages. Cells were a homogeneous population of fibroblasts not positive for the macrophage-specific antigens CD68 and CD14. For cholesterol-depletion experiments, 2 % methyl-β-cyclodextrin was added for 1–2 h.

Tonsillar T-cells were isolated from human palatine tonsils as described previously [9]. T-cells obtained after lysis of sheep red blood cells were > 96 % pure, as estimated by use of flow-cytometry analysis with monoclonal antibodies specific to CD19, CD3 and CD14. The human lymphocytic T-cell lines HUT 78 and Jurkat (ATCC, kindly provided by Dr O. Werdelin, University of Copenhagen, Copenhagen, Denmark) were cultured in RPMI 1640 with 10 % foetal calf serum, antibiotics (1 μl/ml Fungizone and 0.75 μl/ml refobacin) and 50 μM 2-mercaptoethanol.

For co-culture experiments, synoviocytes were seeded in flat-bottomed 12-well culture plates (10^5 cells/well), precoated with 0.5 % gelatin in PBS (pH 7.4). Cells were treated with methyl-β-cyclodextrin either as native cells or after fixation (2 % paraformaldehyde in PBS, pH 7.4, for 15 min followed by three washes in PBS). Tonsillar lymphocytes, resuspended at a final concentration of 5×10^5 cells/ml serum-free AIM-V medium and interleukin-2 (100 units/ml)/concanavalin A (10 ng/ml), were added to the adherent cells and co-cultured for periods of 2 h–2 days. HUT 78 and Jurkat cells were used under similar conditions, but without interleukin-2 and mitogens, in a concentration of 3×10^5 cells/ml. After the co-culture period, lymphocytes were harvested by vigorous pipetting and stained for flow cytometry.

Immunofluorescence staining and confocal laser microscopy

Synoviocytes are distinguishable from lymphocytes by FACS light scattering. To ensure that detectable CD13 expression was truly of lymphocytic origin, two-colour staining with FITC-conjugated anti-CD3 and phycoerythrin-conjugated anti-CD13 was performed in experiments with tonsillar T-cells. Lymphocytes were resuspended at a concentration of 10^6 cells/well. Double staining was performed at 20 °C for 20 min. After two cold washes with PBS containing 0.1 % sodium azide, the cells were fixed using 1 % paraformaldehyde. Fluorescence analyses were performed on a Becton Dickinson FACScan; 5000 cells/sample were counted. Data were subsequently processed using the Lysis program (Becton Dickinson).

For laser-scanning microscopy, synoviocytes grown in chamber slides (Nunc, Wiesbaden, Germany) were fixed with 4 % paraformaldehyde in PBS (pH 7.2). After permeabilization (0.5 % Nonidet P-40 for 10 min) and quenching with 50 mM ammonium acetate, cells were washed and stained with anti-CD13 monoclonal antibody (clone Leu-M7) or an isotype control at 20 °C for 30 min, followed by three washing steps and incubation with a FITC-conjugated secondary antibody. Cells were stained with the polyclonal anti-caveolin antibody overnight, followed by three washing steps, incubation with an anti-rabbit secondary antibody, washing and mounting. Laser-scanning confocal microscopy was performed using a Zeiss LSM 410 microscopic system (Carl Zeiss, Jena, Germany). Image processing was done by using the co-localization program of the LSM 410 by selecting pixels of the same intensity higher than the relative brightness of 20 %.

Electron microscopy

Unless stated, all procedures were performed at 4 °C. For ultrastructural analysis, synoviocytes depleted of cholesterol for 1 h at 37 °C by 2 % methyl-β-cyclodextrin and control cells cultured in parallel were fixed in 2.5 % glutaraldehyde in 0.1 M

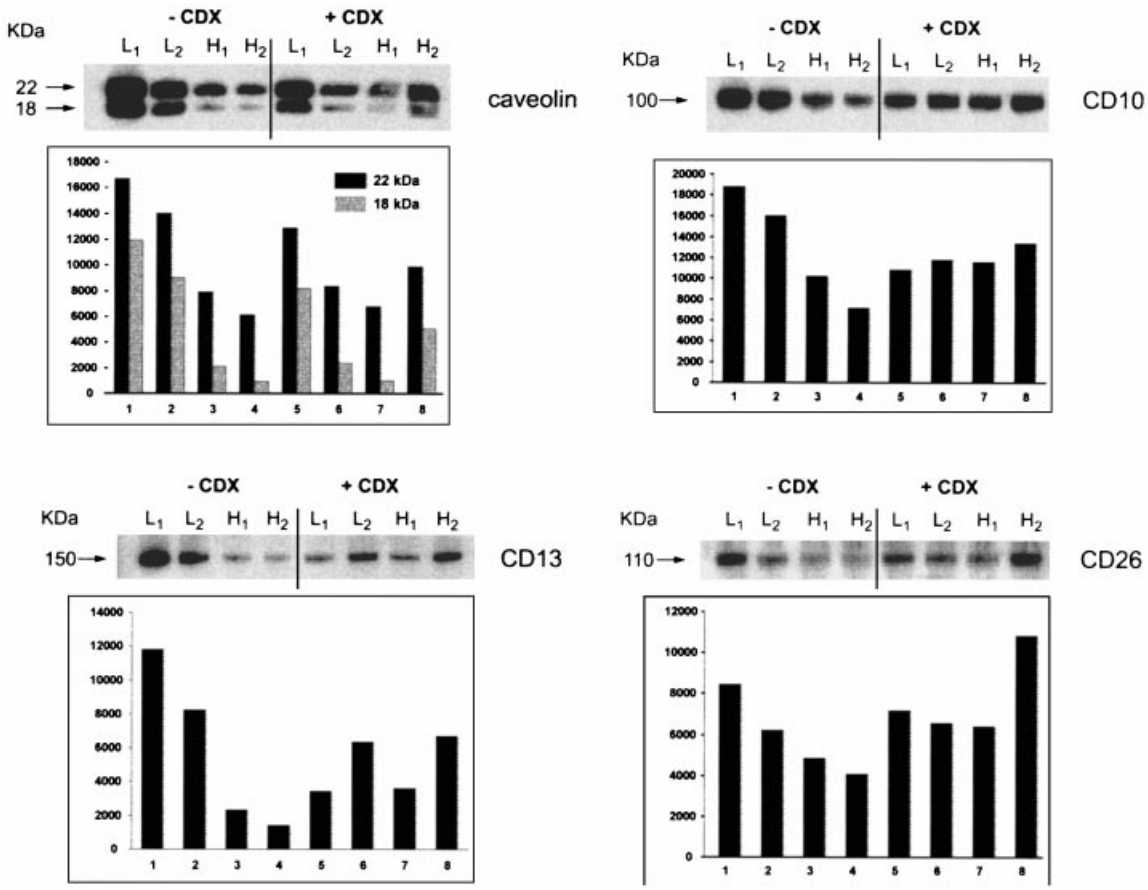

Figure 1 Aminopeptidase N/CD13, dipeptidyl peptidase IV/CD26 and neprilysin/CD10 of fibroblast-like synoviocytes reside in lipid rafts

Control synoviocytes (−CDX) and cells treated with methyl-β-cyclodextrin (+CDX) were homogenized, extracted with ice-cold Triton X-100, and subjected to sucrose-gradient centrifugation as described in the Experimental section. Two low-density fractions (L_1 and L_2, containing the 5/30% sucrose interface) and two high-density fractions (H_1 and H_2, containing the 40% sucrose fraction) were analysed by SDS/PAGE followed by Western blotting to show the distribution of caveolin, aminopeptidase N/CD13, neprilysin/CD10 and dipeptidyl peptidase IV/CD26 in lipid rafts. In the caveolin panel the dark bars represent the 22 kDa form and the shaded bars represent the 18 kDa form of the molecule. Arbitrary units from densitometric scanning are shown. The Figure shows one representative series of experiments out of three performed.

sodium phosphate, pH 7.2 (PB) for 15 min. After post-fixation in 1% osmium tetroxide in PB for 15 min and treatment with 1% uranyl acetate for 1 h at room temperature, the cells were dehydrated and embedded in Epon as described previously [18,19].

For pre-embedding immunogold labelling of aminopeptidase N/CD13 and caveolin, the cells were fixed in freshly prepared 4% paraformaldehyde in PB for 2 h. After three 10 min rinses in PB, the cells were washed twice in 0.05 M Tris/HCl/0.15 M NaCl, pH 7.4 (TBS) before treatment with 3% BSA in TBS for 30 min. The cells were incubated with primary antibodies (rabbit anti-aminopeptidase N or rabbit anti-caveolin) for 20 h at 4 °C and 2 h at room temperature. After three 10 min washes in TBS, the cells were incubated for 1 h at room temperature with secondary antibody (goat anti-rabbit IgG conjugated with 7 nm gold particles [20]) and then washed twice in TBS and in PBS. The cells were finally fixed, post-fixed and embedded in Epon as described above. In labelling experiments for caveolin, the cells were permeabilized with 0.05% saponin prior to labelling, and saponin was included in all subsequent incubations and washing steps. In double-labelling experiments with both aminopeptidase N/CD13 and caveolin, fixation in 2% paraformaldehyde and 0.1% glutaraldehyde for 2 h at room temperature was used to destroy the antigenicity of the antibodies of the first labelling. In all experiments, controls omitting the relevant primary antibodies were included.

For quantitative analyses of gold particles and caveolae, countings were performed on 100 or 200 comparable plasma membrane stretches at a 30000 × magnification using a monitor and an MTI CDD 72 video camera.

Subcellular fractionation

Raft membrane microdomains were isolated using flotation on discontinuous sucrose gradients [21]. In brief, adherent cells (5×10^7) were washed with ice-cold PBS and lysed for 30 min on ice in 1% Triton X-100 in MNE buffer (150 mM NaCl/2 mM EDTA/25 mM Mes, pH 6.5) containing a protease inhibitor mixture. The lysis solution was homogenized further, and nuclei and cellular debris were pelleted by centrifugation at 10000 ***g*** for 30 min. For sucrose-gradient centrifugation, 1 ml of the cleared supernatant was mixed with 1 ml of 85% sucrose in MNE buffer and transferred to the bottom of a centrifuge tube. The diluted lysate was overlaid with 2 ml of 30% sucrose and 1 ml of 5% sucrose in MNE buffer. The samples were centrifuged in an SW55 rotor at 200000 ***g*** at 4 °C for 16 h. Four fractions of 1 ml

were collected from the top of the gradient: two low-density fractions containing lipid rafts (L_1, L_2, containing the 5/30% sucrose interface), and two high-density fractions (H_1, H_2, containing the 40% sucrose fraction).

Functional assay for aminopeptidase activity

Aminopeptidase activity was determined spectrophotometrically at 390 nm using 1.5 mM Ala-*p*-nitroanilide as substrate. Assays were performed with intact confluent cell monolayers, grown in 48-well plates. Cells were rinsed three times and incubated with substrate for 30–40 min at 37 °C in 67 mM Na_2HPO_4/KH_2PO_4, pH 7.2, and the amount of *p*-nitroaniline formed was measured in the supernatant. Measurements were performed in quadruplicate with cell-free and substrate-free controls incubated in parallel. Cells were detached and counted. Enzyme activities were expressed as pkat/10^6 cells.

Western-blot analysis

Samples were electrophoresed on NuPAGE gels as recommended by the manufacturer (NOVEX™ Electrophoresis GmBH, Frankfurt/Main, Germany). Transfer to nitrocellulose (ECL, Amersham Pharmacia Biotech, Braunschweig, Germany) was performed using a semi-dry Fastblot™ apparatus (Biometra, Goettingen, Germany) according to the manufacturer's protocol. The nitrocellulose was blocked with 5% dry milk powder in TBS-T buffer [10 mM Tris/HCl (pH 7.5)/100 mM NaCl/0.1% Tween-20] for 1 h, and then incubated with the first antibody in a blocking solution containing 1% dry milk powder at room temperature for 1 h. The blots were washed three times with TBS-T buffer. Following incubation with the appropriate horseradish peroxidase-conjugated secondary antibody for 1 h, blots were developed using an ECL-based system (Amersham Pharmacia Biotech). Densitometry was performed using the SCANPACK II software (Biometra). For CD13 detection in Western blots a mixture of the monoclonal antibody clones SJ1D1, MY7, Leu-M7 and WM15 (each 1:1000) was used. For detection of dipeptidyl peptidase IV and caveolin, polyclonal antibodies were used at a dilution of 1:250.

Other methods

The free cholesterol concentration in synoviocyte homogenates was determined spectrophotometrically by a cholesterol oxidase/peroxidase assay [22]. Protein concentration was determined using the BCA protein assay reagent kit (Pierce, Rockford, IL, U.S.A.).

RESULTS

Synoviocyte aminopeptidase N/CD13, dipeptidyl peptidase IV/CD26 and neprilysin/CD10 reside in lipid rafts that are sensitive to cholesterol depletion

Figure 1 is one representative experiment out of three performed showing the distribution of caveolin, a cytosolic coat protein known to be associated with caveolae [23,24], and aminopeptidase N/CD13, dipeptidyl peptidase IV/CD26 and neprilysin/CD10 in the low-density (L_1 and L_2) and high-density (H_1 and H_2) fractions of a sucrose gradient following a detergent extraction at low temperature. Caveolin (both the normal 22 kDa polypeptide as well as a band of 18 kDa probably representing the β-isoform of the protein [25]) was predominantly present in the two low-density fractions, as should be expected for a marker protein for lipid rafts. The membrane peptidases were likewise mainly seen in the low-density fractions; thus aminopeptidase N/CD13 was almost exclusively confined to the L_1 and L_2 fractions, whereas 30–40% of dipeptidyl peptidase IV/CD26 and neprilysin/CD10 were partitioned in the high-density fractions.

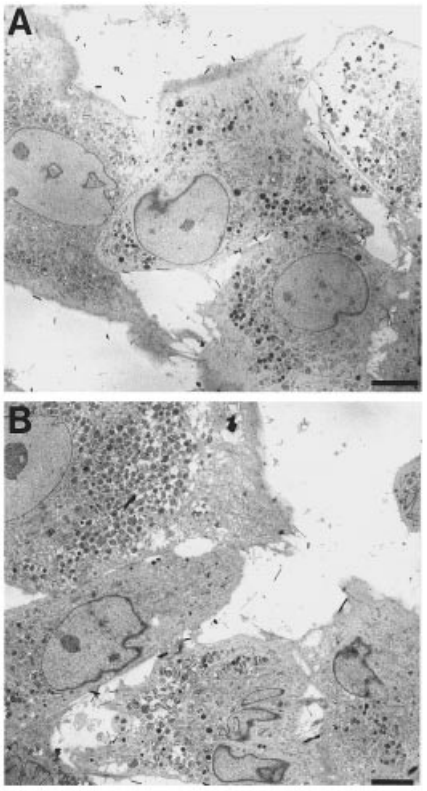

Figure 2 General morphology of synoviocytes

Low-magnification electron micrograph of synoviocytes grown in the absence (**A**) or presence (**B**) of 2% methyl-β-cyclodextrin for 1 h. The general morphology of the cells was unaffected by the treatment. Scale bars, 5 μm.

Treatment with 2% methyl-β-cyclodextrin for 60 min depleted synoviocytes of 60–70% of the cholesterol (results not shown) without affecting the overall cellular ultrastructure (Figure 2). As shown in Figure 1, the treatment diminished the relative amounts of caveolin as well as of the three membrane peptidases in the low-density fractions of the sucrose gradient to about 50%. Taken together, these results indicate that in synoviocytes most of aminopeptidase N/CD13 and the major parts of dipeptidyl peptidase IV/CD26 and neprilysin/CD10 reside in lipid raft microdomains. Importantly, cholesterol depletion did not affect the synoviocyte Ala-*p*-nitroanilide-hydrolysing activity. Thus control adherent native cells and paraformaldehyde-fixed cells had an activity of 1597 ± 577 pkat/10^6 cells (mean $\pm$ S.D.), whereas the corresponding activity of cholesterol-depleted cells was 97.3 ± 10.1% of the controls, showing that cholesterol depletion did not itself cause a loss of aminopeptidase N/CD13 from the synoviocytes.

Subcellular localization of synoviocyte caveolin, aminopeptidase N/CD13 and dipeptidyl peptidase IV/CD26

Figure 3 shows the distribution of aminopeptidase N/CD13 and caveolin in adherent subconfluent monolayers of synoviocytes using laser-scanning microscopy, and indicates a partial co-

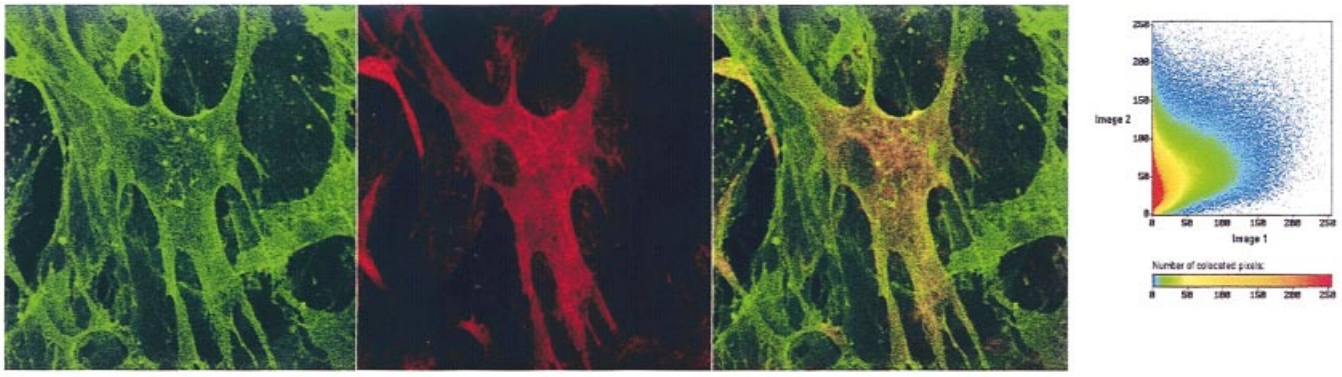

Figure 3 Partial co-localization of aminopeptidase N/CD13 and caveolin on synoviocytes

After fixation and permeabilization subconfluent cell cultures were indirectly stained with a CD13-specific monoclonal antibody (green), followed by indirect staining for caveolin (red). In the merged picture, co-localization is visualized as yellow. Quantification of pixel co-localization is also shown.

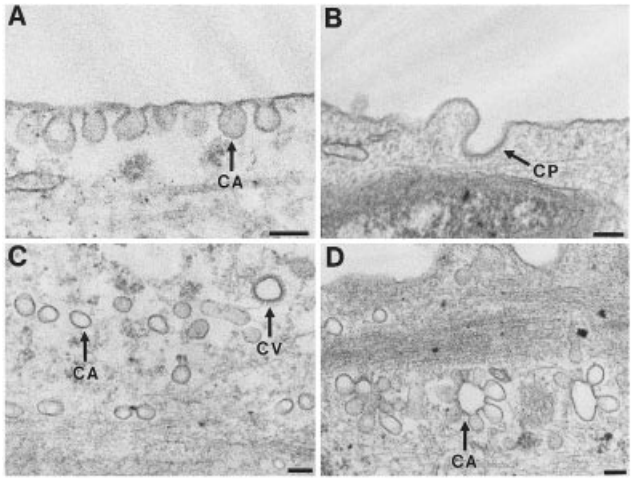

Figure 4 The ultrastructure of synoviocytes is affected by cholesterol depletion

Caveolae (CA) are seen as single flask-shaped invaginations at the cell surface (**A**), as vesicle-like structures distinct from coated vesicles (CV) inside the cell (**C**), and as conglomerates of several caveolae organized in a rosette-like pattern (**D**). Cholesterol depletion greatly reduced the number of all the caveolae structures (**B**), but did not affect coated pits (CP). Scale bars, 100 nm.

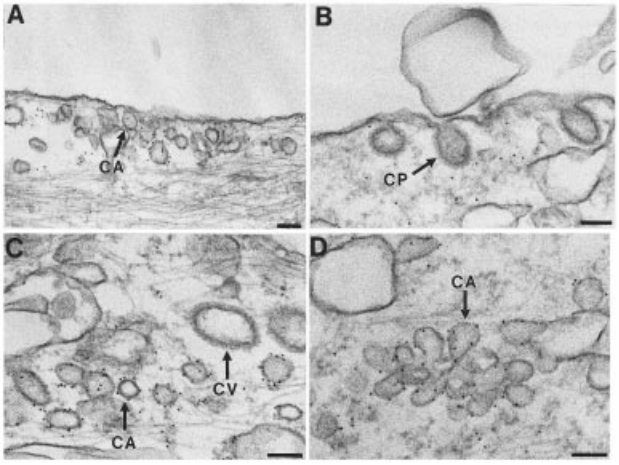

Figure 5 Immunogold labelling of caveolin in control and cholesterol-depleted synoviocytes

In control cells (**A**, **C**, **D**) caveolin is localized in single flask-shaped caveolae (CA) at the cell surface (**A**) and in intracellular vesicle-like and rosette-like structures (**C**, **D**), demonstrating these to be of caveolar origin. No specific labelling of coated vesicles (CV) was observed. In cholesterol-depleted cells (**B**), caveolin labelling was confined to flat stretches of plasma membrane and the underlying cytoplasm. CP, coated pit. Scale bars, 100 nm.

localization of the two proteins. At the ultrastructural level many single caveolae were seen at the cell surface, exhibiting the typical flask-shaped morphology, but vesicle-like caveolae and conglomerates consisting of several caveolae organized in a characteristic rosette pattern were also frequently observed lying deeper in the cytoplasm (Figure 4). Cholesterol depletion reduced dramatically ($> 90\%$ by quantitative analysis) the number of caveolae at the cell surface as well as those located intracellularly, whereas clathrin-coated pits were unaffected by cholesterol depletion (Figure 4B).

By immunogold electron microscopy, an antibody to caveolin specifically labelled the caveolae at the cell surface, the intracellular vesicle-like structures and the caveolae rosettes (Figure 5), demonstrating that the latter are indeed of caveolar origin. After cholesterol depletion caveolin was found on flat stretches of the cell surface or scattered in the cytoplasm underneath the plasma membrane (Figure 5B).

By immunogold electron microscopy, aminopeptidase N/CD13 was found occasionally in caveolae at the cell surface, but interestingly, the intracellular vesicle-like structures and caveolae rosettes were much more frequently labelled than the single caveolae at the cell surface (Figure 6). Thus by quantitative analysis, the major part (approx. 60%) of the total cellular labelling for aminopeptidase N/CD13 was seen in the intracellular vesicle-like caveolae and caveolae rosettes. Since aminopeptidase N/CD13 labelling was performed on whole unpermeabilized cells after paraformaldehyde fixation, these intracellular structures were freely connected to the cell surface despite their location deep within the cytoplasm. At the cell surface, aminopeptidase N/CD13 was most frequently observed over non-caveolar stretches of flat membrane where it typically

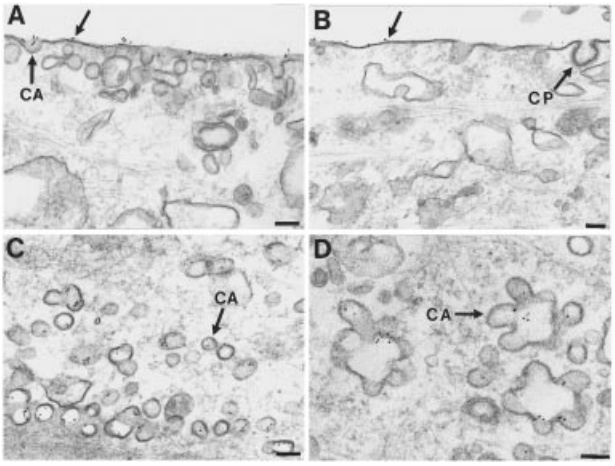

Figure 6 Immunogold labelling of aminopeptidase N/CD13 in control and cholesterol-depleted synoviocytes

At the cell surface of control cells, aminopeptidase N/CD13 is found mainly on flat stretches of membrane (arrow), but also in caveolae (CA; **A**). However, the labelling is more intense in intracellular vesicle-like structures (**C**) and in particular in caveolae rosettes (**D**). In cholesterol-depleted cells (**B**), labelling is observed almost exclusively at the cell surface (arrow). Note that labelling is absent from coated pits (CP) in (**B**). Scale bars, 100 nm.

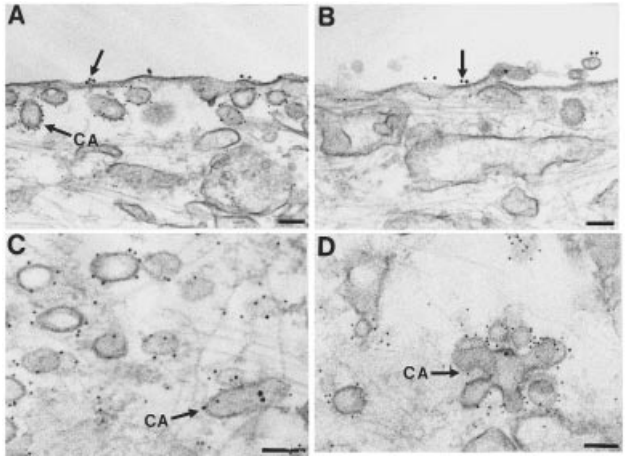

Figure 8 Immunogold double labelling of caveolin and aminopeptidase N/CD13 in control and cholesterol-depleted synoviocytes

At the cell surface of control cells (**A**), aminopeptidase N/CD13 (13 nm gold particles) is seen on flat stretches of membrane whereas caveolin (7 nm gold particles) is found in caveolae (CA). Co-localization is mainly observed in intracellular vesicle-like caveolae (CA; **C**) and in caveolae rosettes (CA; **D**). In cholesterol-depleted synoviocytes (**B**), aminopeptidase N/CD13 is seen at the cell surface and caveolin is scattered in the underlying cytoplasm. Scale bars, 100 nm.

appeared in clusters (Figures 6A and 7), indicating a microdomain-restricted localization. The size of these flat microdomains was 111 ± 51 nm (mean $\pm$ S.D.; $n = 100$).

After cholesterol depletion, the surface labelling for aminopeptidase N/CD13 was no longer clustered in microdomains but appeared evenly distributed (Figure 6B). Aminopeptidase N/CD13 was not seen intracellularly by the pre-embedding immunogold labelling technique, indicating that the intracellular pool of the peptidase had either been redistributed to the surface or become inaccessible to the antibody (Figure 6B). When using post-embedding immunogold labelling, some intracellular aminopeptidase N/CD13 could be detected in ultracryosections after cholesterol depletion, but it was no longer associated with identifiable membrane structures (results not shown). However, the fact that the Ala-*p*-nitroanilide-hydrolysing activity of the cells was unchanged after cholesterol depletion suggests that this intracellular labelling only represents a minor part of the total cellular amount of aminopeptidase N/CD13.

Immunogold double labelling confirmed that aminopeptidase N/CD13 largely resides in non-caveolar regions of the cell surface, whereas the aminopeptidase N/CD13-positive intracellular structures are clearly of caveolar origin (Figure 8).

Taken together, the ultrastructural and biochemical evidence shows that aminopeptidase N/CD13 in synoviocytes is clustered in caveolae/rafts. Interestingly, the cholesterol-dependent clustering is seen predominantly in deep-lying yet surface-connected vesicle-like caveolae and caveolae rosettes, and in flat areas of the plasma membrane. Only to a lesser extent is aminopeptidase N/CD13 localized in single caveolae at the cell surface. Figure 9 shows the localization of dipeptidyl peptidase IV/CD26. Like aminopeptidase N/CD13, this peptidase was seen mainly in flat patches at the cell surface and in the intracellular caveolae rosettes, indicating that both peptidases reside in these membrane domains.

Cholesterol depletion of synoviocytes reduces their ability to stimulate lymphocytic expression of aminopeptidase N/CD13

To study the possible significance of the observed caveolae/raft localization of the ectopeptidases in synoviocytes, we next examined the effect of methyl-β-cyclodextrin on a cellular function where aminopeptidase N/CD13 has previously been implicated, namely the ability to rapidly induce the ectopeptidase on CD13-negative lymphocytes in co-culture with synoviocytes [9].

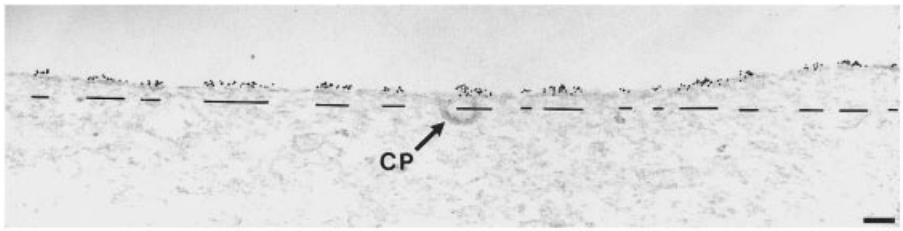

Figure 7 Microdomain clustering of aminopeptidase N/CD13 at the synoviocyte cell surface

Immunogold labelling at the cell surface is seen mainly in clusters of several particles on flat stretches of membrane. Note the lack of labelling of the coated pit (CP). Scale bar, 100 nm.

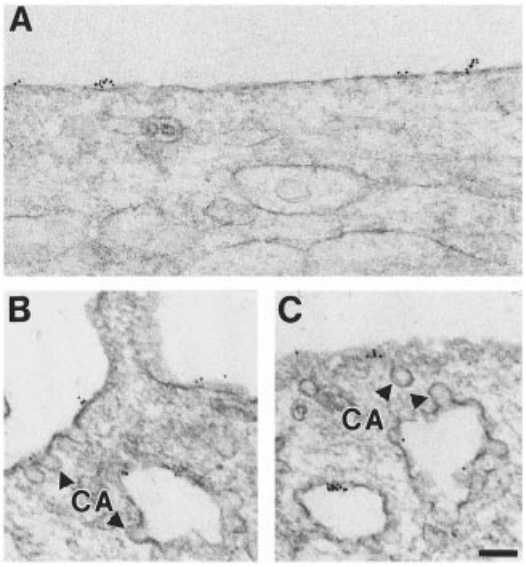

Figure 9 Immunogold localization of dipeptidyl peptidase IV/CD26 in synoviocytes

Immunogold labelling of dipeptidyl peptidase IV/CD26. Labelling is seen in clusters on flat patches of the cell surface and in intracellular rosettes of caveolae (CA). Scale bar, 100 nm.

In such co-cultures, tonsillar T-cells adhered in a comparable manner to native, fixed and methyl-β-cyclodextrin-treated synoviocytes after just 20 min of co-culture (results not shown). Mitogens could augment the adhesion of tonsillar T-cells and also enhanced the lymphocytic expression of aminopeptidase N/CD13, as described previously [9]. Table 1 shows the time course of lymphocytic CD13 expression after cell–cell contact of tonsillar T-cells on paraformaldehyde-fixed synoviocytes. As shown in Table 1, pretreatment of synoviocytes with methyl-β-cyclodextrin for 2 h greatly diminished their ability to induce an early CD13 expression on tonsillar T-lymphocytes. Similar results were obtained with HUT 78 T-cells (Table 2) and with Jurkat T-cells (results not shown).

DISCUSSION

Previous studies from several laboratories have implicated aminopeptidase N/CD13 in various types of inflammatory processes involving the interaction between synoviocytes, monocytes and lymphocytic cells [26]. To gain more insight into this, we studied in closer detail the subcellular distribution of this membrane protein in synoviocytes. We observed that aminopeptidase N/CD13 predominantly resides in the low-temperature detergent-insoluble membrane fraction, a hallmark of glycolipid and cholesterol-rich membrane microdomains commonly referred to as lipid rafts. Neprilysin/CD10 and dipeptidyl peptidase IV/CD26, two other membrane peptidases, were also found in lipid rafts, albeit to a lesser extent. We have previously reported aminopeptidase N/CD13 to be a raft component in monocytes [27], and aminopeptidase N/CD13 and dipeptidyl peptidase IV/CD26 to be raft constituents of the brush border membrane of intestinal enterocytes [28]. However, in other tissues such as kidney [29] and brain [14], aminopeptidase N/CD13 is fully detergent-soluble, indicating that raft association may rely on cell-type-specific factors, for instance the lipid composition of the cell membrane.

In synoviocytes the presence in the biochemically defined lipid raft fraction at least partially correlated with an ultrastructural presence in caveolae, a subcellular localization not previously reported for a transmembrane ectopeptidase. Surprisingly, the highest density of aminopeptidase N/CD13 labelling was found

Table 1 Time course of aminopeptidase N/CD13 expression on tonsillar lymphocytes following adhesion to fibroblast-like synoviocytes

Synoviocytes were fixed with paraformaldehyde (−) and additionally treated with 2% methyl-β-cyclodextrin (+) and washed thoroughly. Tonsillar T-cells adhered to synoviocytes in the absence (−) or presence (+) of the T-cell-specific mitogen concanavalin A for varying periods of time. At the end of the adhesion period lymphocytes were harvested and stained for aminopeptidase N/CD13 expression and for CD3 using directly labelled antibodies. Lymphocyte CD13 expression is given as the percentage of CD3-positive cells.

	Lymphocyte CD13 expression (% of CD3-positive cells)											
Incubation time (h) ...	2				24				48			
Methyl-β-cyclodextrin ...	−		+		−		+		−		+	
Concanavalin A ...	−	+	−	+	−	+	−	+	−	+	−	+
CD13 expression	13.2±3.0	37.0±14.0	4.2±2.4	12.0±8.5	20.2±5.4	43.4±9.0	8.8±5.7	12.6±5.5	24.0±3.5	76.2±16.0	8.0±4.0	26.5±13.4

Table 2 Time course of aminopeptidase N/CD13 expression on HUT 78 T-cells following adhesion to fibroblast-like synoviocytes

Synoviocytes were treated as described in Table 1. At the end of the adhesion period lymphocytes were harvested and stained for aminopeptidase N/CD13 expression (given as mean fluorescence intensity).

	Aminopeptidase N/CD13 expression (mean fluorescence intensity)							
Incubation time (h) ...	1		2		24		48	
Methyl-β-cyclodextrin ...	−	+	−	+	−	+	−	+
CD13 expression	71	19	118	52	367	128	394	362

in deeper-lying rather than surface-localized caveolae; in fact, well over half the total amount of aminopeptidase N/CD13 was present in these structures. At the cell surface, the peptidases were typically clustered on flat stretches of the plasma membrane ranging in size from about 60 to 160 nm, indicating that lipid rafts are able to form non-caveolar microdomains of this size. The question concerning the size of lipid rafts *in vivo* has been debated over the past few years since too small a size for accomodation of a minimum number of proteins would argue against rafts playing a functional role as lateral sorting platforms [30,31]. By fluorescence resonance energy transfer (FRET) and chemical cross-linking studies of glycosylphosphatidylinositol-linked proteins, raft microdomains were reported to be 70 nm or less [32], and to harbour about 15 protein molecules per raft [33]. Rafts of a comparable size (radius 26 nm) were observed recently by a novel microscopic technique, based on viscous drag measurements of glycosylphosphatidylinositol-linked proteins [34], but other investigators have failed to observe stable rafts by the FRET technique [35–37]. In the present paper stable rafts could be directly visualized at the surface of fixed cells by immunogold electron microscopy of a transmembrane raft protein. The range in their calculated size implies that lipid rafts may be dynamic structures capable of becoming large enough to accomodate the complex trafficking and signalling functions ascribed to them [12,15,38].

The overall steady-state distribution between flat lipid raft microdomains at the cell surface and intracellular caveolae most probably reflects dynamic bidirectional trafficking between the surface and interior of the cell, enabling the synoviocyte to regulate its surface expression of peptidases together with other caveolae-associated proteins. Being surface connected, however, the large number of intracellular caveolae may well be functional rather than merely a passive reservoir. In endothelial cells, a vesiculo-vacuolar organelle morphologically related to the caveolae rosettes has been proposed to provide a transcellular pathway for macromolecules [39]. A possible function of peptidases in intracellular synoviocyte caveolae could be to process hormonal signals, for instance during cell–cell contact. Here, a function of the caveolae rosettes could be to provide an optimal, 'unstirred' environment with a high surface/volume ratio. Interestingly, in a recent study caveolin was shown to relocalize to areas of cell–cell contact when fibroblasts become confluent, and caveolae to become grouped together in patches containing 10–100 densely packed units [40], and a similar enrichment in areas of cell–cell contact has also been described for aminopeptidase N/CD13 in cultured melanoma cells [41]. Many of the known physiological substrates of aminopeptidase N/CD13 act via G-protein-coupled receptors known to be caveolae-associated in other cell types [15], and here aminopeptidase N/CD13 might act as a negative regulator by cleavage of substrate peptides. However, a more direct role in signal transduction with membrane peptidases acting as ligands is also conceivable, as suggested by reports that cross-linking of aminopeptidase N/CD13 in monocytes increases intracellular free calcium and results in activation of mitogen-activated protein kinases [42]. Likewise, dipeptidyl peptidase IV/CD26 has been shown to be directly involved in early phosphorylation events not only in T-cells [43], but also in non-haematopoetic cells, such as hepatocarcinoma [44]. Neprilysin/CD10 was recently reported to be raft-associated in pre-B cells [45], and proteins associated with it, such as the 56 kDa Lyn, a Src-related kinase, become tyrosine phosphorylated *in vitro* when co-immunoprecipitated with the peptidase [45,46].

In summary, we propose caveolae/rafts to be peptidase-rich 'hot spots' in fibroblast-like synoviocytes, likely to be of importance in cell–cell interactions. Future work will have to elucidate further the functioning and dynamics of these membrane microdomains.

We are especially grateful to Dr Vera John (Department of Rheumatology, Children's Hospital, Halle, Germany) and Dr Joerg Brandt (Department of Orthopaedics, Martin Luther University, Halle, Germany) for supplying us with synovectomy tissue, to G. Helbing and K. Bornschein for the excellent technical assistance and to Bettina Hause (Leibnitz Institute of Plant Biochemistry, Halle, Germany) for help with laser scanning microscopy. Professor Hans Sjöström and Professor Ove Norén are thanked for valuable discussions about the manuscript. This investigation was part of the Danish Biotechnology programme and was supported by grants from the Novo-Nordic Foundation, the Danish Cancer Society, the Danish Medical Research Council and the Deutsche Forschungsgemeinschaft (SFB 387).

REFERENCES

1 Firestein, G. S. (1996) Invasive fibroblast-like synoviocytes in rheumatoid arthritis. Passive responders or transformed aggressors? Arthritis Rheum. **39**, 1781–1790
2 Bathon, J. M., Proud, D., Mizutani, S. and Ward, P. E. (1992) Cultured human synovial fibroblasts rapidly metabolize kinins and neuropeptides. J. Clin. Invest. **90**, 981–991
3 Schwachula, A., Riemann, D., Kehlen, A. and Langner, J. (1994) Characterization of the immunophenotype and functional properties of fibroblast-like synoviocytes in comparison to skin fibroblasts and umbilical cells. Immunobiology **190**, 67–92
4 Stange, T., Kettmann, U. and Holzhausen, H.-J. (1996) Immunoelectron microscopic single and double labeling of aminopeptidase N (CD13) and dipeptidyl peptidase IV (CD26). Acta Histochem. (Jena) **98**, 323–331
5 Norén, O., Sjöström, H. and Olsen, J. (1997) Aminopeptidase N. In Cell-Surface Peptidases (Kenny, A. J. and Bousted, C. M., eds.), pp. 175–191, Bios Scientific Publishers, Oxford
6 Matsas, R., Stephenson, S. L., Hryszko, J., Kenny, A. J. and Turner, A. J. (1985) The metabolism of neuropeptides. Phase separation of synaptic membrane preparations with Triton X-114 reveals the presence of aminopeptidase N. Biochem. J. **231**, 445–449
7 Kokkonen, J. O., Kuoppala, A., Saarinen, J., Lindstedt, K. A. and Kovanen, P. T. (1999) Kallidin- and bradykinin-degrading pathways in human heart: degradation of kallidin by aminopeptidase M-like activity and bradykinin by neutral endopeptidase. Circulation **99**, 1984–1990
8 Weber, M., Uguccioni, M., Baggiolini, M., Clark-Lewis, I. and Dahinden, C. A. (1996) Deletion of the NH2-terminal residue converts monocyte chemotactic protein 1 from an activator of basophil mediator release to an eosinophil chemoattractant. J. Exp. Med. **183**, 681–685
9 Riemann, D., Kehlen, A., Thiele, K., Löhn, M. and Langner, J. (1997) Induction of aminopeptidase N/CD13 on human lymphocytes after adhesion to fibroblast-like synoviocytes, endothelial cells, epithelial cells, and monocytes/macrophages. J. Immunol. **158**, 3425–3432
10 Barrett, A. J. (1998) Neprilysin. In Handbook of Proteolytic Enzymes (Barrett, A. J., Rawlings, N. D. and Woessner, J. F., eds.), pp. 1080–1085, Academic Press, London
11 De Meester, I., Korom, S., Van Damme, J. and Scharpe, S. (1999) CD26, let it cut or cut it down. Immunol. Today **20**, 367–375
12 Simons, K. and Ikonen, E. (1997) Functional rafts in cell membranes. Nature (London) **387**, 569–572
13 Brown, D. A. and London, E. (1998) Functions of lipid rafts in biological membranes. Annu. Rev. Cell Biol. **14**, 111–136
14 Hooper, N. M. (1999) Detergent-insoluble glycosphingolipid/cholesterol-rich membrane domains, lipid rafts and caveolae. Mol. Membr. Biol. **16**, 145–156
15 Anderson, R. G. W. (1998) The caveolae membrane system. Annu. Rev. Biochem. **67**, 199–225
16 Okamoto, T., Schlegel, A., Scherer, P. E. and Lisanti, M. P. (1998) Caveolins, a family of scaffolding proteins for organizing 'preassembled signaling complexes' at the plasma membrane. J. Biol. Chem. **273**, 5419–5422
17 Hansen, G. H., Niels-Christiansen, L.-L., Poulsen, M. D., Norén, O. and Sjöström, H. (1994) Distribution of three microvillar enzymes along the small intestinal crypt-villus axis. J. Submicrosc. Cytol. Pathol. **26**, 453–460
18 Hansen, G. H., Belhage, B., Schousboe, A. and Meier, E. (1987) Temporal development of GABA agonist induced alterations in ultrastructure and GABA receptor expression in cultured cerebellar granule cells. Int. J. Dev. Neurosci. **5**, 263–269
19 Hansen, G. H., Hösli, E., Belhage, B., Schousboe, A. and Hösli, L. (1991) Light and electron microscopic localization on cultured cerebellar granule cells and astrocytes using immunohistochemical techniques. Neurochem. Res. **16**, 341–346
20 Hansen, G. H., Wetterberg, L.-L., Sjöström, H. and Norén, O. (1992) Immunogold labelling is a quantitative method as demonstrated by studies on aminopeptidase N in microvillar membrane vesicles. Histochem. J. **24**, 132–136

21 Kabouridis, P. S., Magee, A. I. and Ley, S. C. (1997) S-acylation of LCK protein tyrosine kinase is essential for its signalling function in T lymphocytes. EMBO J. **16**, 4983–4998

22 Gamble, W., Vaughan, M., Kruth, H. S. and Avignan, J. (1978) Procedure for determination of free and total cholesterol in micro- or nanogram amounts suitable for studies with cultured cells. J. Lipid Res. **19**, 1068–1070

23 Rothberg, K. G., Heuser, J. E., Donzell, W. C., Ying, Y. S., Glenney, J. R. and Anderson, R. G. (1992) Caveolin, a protein component of caveolar membrane coats. Cell **68**, 673–682

24 Sargiacomo, M., Sudol, M., Tang, Z. I. and Lisanti, M. P. (1993) Signal transduction molecules and glycosyl-phosphatidylinositol-linked proteins form a caveolin-rich insoluble complex in MDCK cells. J. Cell Biol. **122**, 789–807

25 Kogo, H. and Fujimoto, T. (2000) Caveolin-1 isoforms are encoded by distinct mRNAs. Identification of mouse caveolin-1 mRNA variants caused by alternative transcription initiation and splicing. FEBS Lett. **465**, 119–123

26 Riemann, D., Kehlen, A. and Langner, J. (1999) CD13 – a cell–cell contact regulated peptidase on lymphocytes and not only a marker in leukemia typing. Immunol. Today **20**, 83–88

27 Santos, A. N., Roentsch, J., Danielsen, E. M., Langner, J. and Riemann, D. (2000) Aminopeptidase N/CD13 is associated with raft membrane microdomains in monocytes. Biochem. Biophys. Res. Commun. **269**, 143–148

28 Danielsen, E. M. (1995) Involvement of detergent-insoluble complexes in the intracellular transport of intestinal brush border enzymes. Biochemistry **34**, 1596–1605

29 Hooper, N. M. and Turner, A. J. (1988) Ectoenzymes of the kidney microvillar membrane. Differential solubilization by detergents can predict a glycosyl-phosphatidylinositol membrane anchor. Biochem. J. **250**, 865–869

30 Hooper, N. M. (1998) Membrane biology: do glycolipid microdomains really exist? Curr. Biol. **8**, R114–R116

31 Jacobson, K. and Dietrich, C. (1999) Looking at lipid rafts? Trends Cell Biol. **9**, 87–91

32 Varma, R. and Mayor, S. (1998) GPI-anchored proteins are organized in submicron domains at the cell surface. Nature (London) **394**, 798–801

33 Friedrichson, T. and Kurchalia, T. V. (1998) Microdomains of GPI-anchored proteins in living cells revealed by cross-linking. Nature (London) **394**, 802–805

34 Pralle, A., Keller, P., Florin, E.-L., Simons, K. and Hörber, J. K. H. (2000) Sphingolipid-cholesterol rafts diffuse as small entities in the plasma membrane of mammalian cells. J. Cell Biol. **148**, 997–1007

Received 10 August 2000/1 November 2000; accepted 5 December 2000

35 Hannan, L. A., Lisanti, M. P., Rodriguez-Boulan, E. and Edidin, M. (1993) Correctly sorted molecules of a GPI-anchored protein are clustered and immobile when they arrive at the apical surface of MDCK cells. J. Cell Biol. **120**, 353–358

36 Kenworthy, A. K. and Edidin, M. (1998) Distribution of a glycosylphosphatidylinositol-anchored protein at the apical surface of MDCK cells examined at a resolution of < 100 Å using imaging fluorescence resonance energy transfer. J. Cell Biol. **142**, 69–84

37 Kenworthy, A. K., Petranova, N. and Edidin, M. (2000) High-resolution FRET microscopy of a cholera toxin B-subunit and GPI-anchored proteins in cell plasma membranes. Mol. Biol. Cell **11**, 1645–1655

38 Simons, K. and Toomre, D. (2000) Lipid rafts and signal transduction. Nat. Rev. Mol. Cell Biol. **1**, 31–39

39 Dvorak, A. M., Kohn, S., Morgan, E. S., Fox, P., Nagy, J. A. and Dvorak, H. F. (1996) The vesiculo-vacuolar organelle (VVO): a distinct endothelial cell structure that provides a transcellular pathway for macromolecular extravasation. J. Leucocyte Biol. **59**, 100–115

40 Volonte, D., Galbiati, F. and Lisanti, M. P. (1999) Visualization of caveolin-1, a caveolar marker protein, in living cells using green fluorescent protein (GFP) chimeras. FEBS Lett. **445**, 431–439

41 Menrad, A., Speicher, D., Wacker, J. and Herlyn, M. (1993) Biochemical and functional characterization of aminopeptidase N expressed by human melanoma cells. Cancer Res. **53**, 1450–1455

42 Santos, A. N., Langner, J., Herrmann, M. and Riemann, D. (2000) Aminopeptidase N/CD13 is directly linked to signal transduction pathways in monocytes. Cell. Immunol. **201**, 22–32

43 Von Bonin, A., Huhn, J. and Fleischer, B. (1998) Dipeptidylpeptidase IV/CD26 on T cells: analysis of an alternative T-cell activation pathway. Immunol. Rev. **161**, 143–153

44 Gaetaniello, L., Fiore, M., De Filippo, S., Pozzi, N., Tamasi, S. and Pignata, C. (1998) Occupancy of dipeptidyl peptidase IV activates an associated tyrosine kinase and triggers an apoptotic signal in human carcinoma cells. Hepatology **25**, 934–942

45 Angelisova, P., Drbal, K., Horejsi, V. and Cerny, J. (1999) Association of CD10/neutral endopeptidase 24.11 with membrane microdomains rich in glycosylphosphatidylinositol-anchored proteins and Lyn kinase. Blood **93**, 1437–1439

46 Ganju, R. K., Shpektor, R. G., Brenner, D. G. and Shipp, M. A. (1996) CD10/neutral endopeptidase 24.11 is phosphorylated by casein kinase II and coassociates with other phosphoproteins including the Lyn-*src*-related kinase. Blood **88**, 4159–4165